Journal of New Materials for Electrochemical Systems 15, 113-121 (2012)

Electrochemical Properties of 4-[(Anthracen -9-ylmethylene)-amino]-1, 5-dimethyl-2-phenyl-1,2-dihydro-pyrazol-3-one at a Platinum Electrode in Acetonitrile Solvent

Abdullah M. Asiri[1,2,*], Ibrahim S. El-Hallag[1,3], A.O. Al-Youbi[2], Khalid A. Alamry[2] and Salman A. Khan[2]

[1]The Center of Excellence for Advanced Materials Research, King Abdulaziz University, Jeddah, P.O. Box 80203, Saudi Arabia
[2]Chemistry Department, Faculty of Science, King Abdulaziz University, P.O. Box 80203, Jeddah, Saudi Arabia
[3]Department of Chemistry, Faculty of Science, Tanta University, 31527 Tanta, Egypt

Received: June 15, 2011, Accepted: November 16, 2011, Available online: December 15, 2011

Abstract: *The electrochemical properties of 4-[(anthracen -9-ylmethylene)-amino]-1, 5-dimethyl-2-phenyl-1,2-dihydro-pyrazol-3-one have been carried out using cyclic voltammetry and convolution - deconvolution voltammetry combined with digital simulation technique at a platinum electrode in 0.1 mol/L tetraethyl ammonium chloride (TEACl) in solvent acetonitrile (CH_3CN). In switching the potential to positive scan, the compound was oxidized by loss of one electron forming radical cataion followed by fast chemical step and the radical cation loss another two electrons producing trication which followed by chemical reaction (ECEEC). The investigated compound was reduced via consumption of two consecutive electrons to form radical anion followed by fast chemical step and the radical anion gain another electron to form dianion followed by chemical step (ECEC mechanism). The electrode reaction pathway and the chemical and electrochemical parameters of the investigated compound were determined using cyclic voltammetry, convolutive voltammetry and chronoamperometry. The Electrochemical data such as a, k_s, E^o , D, and k_c of the investigated pyrazole derivative were evaluated expeimentally and verified via digital simulation technique Electrochemical behaviour of the pyrazole compound under consideration was presented and discussed.*

Keywords: 1, 5-dimethyl-2-phenyl-1,2-dihydro-pyrazol-3-one, Cyclic voltammetry, Convolutive voltammetry, Digital simulation

1. INTRODUCTION

Pyrazole refers to the class of simple aromatic ring organic compounds of the heterocyclic series characterized by a 5-membered ring structure composed of three carbon atoms and two nitrogen atoms in adjacent positions. Being so composed and having pharmacological effects on humans, they are classified as alkaloids, although they are rare in nature. In 1959, the first natural pyrazole, 1-pyrazolyl-alanine, was isolated from seeds of watermelons [1]. Pyrazole derivatives have a long history of application in agrochemicals and pharmaceutical industry as herbicides and active pharmaceuticals. The recent success of pyrazole COX-2 inhibitor has further highlighted the importance of these heterocyclic rings in medicinal chemistry. A systematic investigation of this class of heterocyclic lead revealed that pyrazole containing pharmacoactive agents play important role in medicinal chemistry**.** The prevalence of pyrazole cores in biologically active molecules has stimulated the need for elegant and efficient ways to make these heterocyclic lead [1].

The main interest towards –pyrazole derivatives relies heavily on their biological activity [2], their use as intermediates in obtaining color photosensitive materials [3-5] as well as toners, inks and other photographic materials [6]. The latter compounds are used as precursors of color photographic light sensitive materials [3], toners, and ink jet printer dyes [6] as well as intermediates in producing solid-state dye-sensitized solar cells (DSSCs)**.**

There is a connection between pharmacological and chemical structure among pyrazole derivatives used in a medical treatment. A chemical division is coincident with a pharmacological division. Pyrazole-5 derivatives are mainly analgesic, antipyretic and less anti-inflammatory and diastolic but pyrazolidyn-3,5-dion derivatives are anti-inflammatory. The main part of non-steroid anti-inflammatory drugs belonging to pyrazolone derivates has a phenyl group at the first position. The activity and toxicity of this

*To whom correspondence should be addressed: Email: aasiri2@gmail.com
Phone: +02-695-2293

drugs are dependent on groups being at the fourth position. For example, the dimethylamino group makes aminophenazon antianalgetic, and yet is also responsible for a big toxicity. Azole derivatives are antimycotic and are ingredients of some ointments and creams. Chemical groups at the fourth position may determine the activity and the toxicity. These days a great attention is paid on a synthesis which is linking pyrazole and ions of platinum Pt(II) and palladium Pd(III) due to anticancer properties but pharmacology is not known very well [7].

Up till now no report on the electrochemistry of 4-[(anthracen -9-ylmethylene)-amino]-1, 5-dimethyl-2-phenyl-1,2-dihydro-pyrazol-3-one via cyclic voltammetry and convolution-deconvolution transforms combined with digital simulation at a Pt electrode in acetonitrile solvent / 0.1M TEACl. So, in the present manuscript we investigated the electrochemical behaviour of pyrazole derivative compound under consideration using cyclic voltammetry and convolution-deconvolution transforms. The experimental chemical and electrochemical parameters was determined and verified via digital simulation method.

2. EXPERIMENTAL

2.1. Chemicals

The investigated 4-[(anthracen -9-ylmethylene)-amino]-1, 5-dimethyl-2-phenyl-1,2-dihydro-pyrazol-3-one was prepared as following:-

A mixture of Anthracene-9-carbaldehyde (0.50 g, 0.0024 mol) and 4-Aminoantipyrine (0.49 g, 0.0024 mol) in ethanol (15 mL) was heated for 3 h. The progress of the reaction was monitored by TLC. The solid that separated from the cooled mixture was collected and recrystallized from a methanol-chloroform mixture (8: 2) to give the title compound (***pyz***).

Yellow solid: Yield: 87%; m.p. 231-232 °C . GC-MS m/z (rel. int.%): 393 (68) $[M+1]^+$,

IR (KBr) νmax cm^{-1}: 3027 (Ar-H), 2874 (C-H), 1636(C=O), 1580(HC=N), 1138 (C-N).

^{1}H NMR (600MHZ, $CDCl_3$) (δ/ppm): 11.06 (s, CH olefinic), 8.98-7.36 (m, 14H Ar-H) 3.23 (s, CH_3), 2.19 (s, CH_3).

^{13}CNMR (600 MHz, $CDCl_3$) δ: 160.84, 157.70, 152.03, 134.75, 131.54, 130.45, 129.32, 129.01, 128.8, 127.11, 126.60, 125.64, 125.22, 124.62, 119.70, 35.78, 10.36.

Anal. calc. for $C_{26}H_{21}N_3O$: C, 79.77, H, 5.41, N, 10.73. Found: C, 79.74, H, 5.38, N, 10.68.

The structures of the investigated pyarazole derivative was shown in scheme 1.

All solvents used in this work were of spectroscopic grade.

Scheme 1.

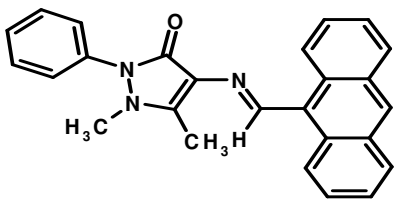

Pyz

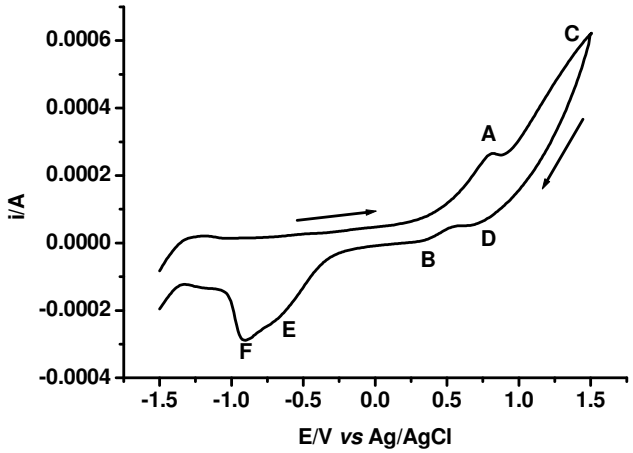

Figure 1. Cyclic voltammogram of 5×10^{-4} M of ***pyz*** in CH_3CN / 0.1M TEACl at scan rate of 0.8 V/s.

2.2. Electrochemical measurements

Cyclic voltammetry and convolution-deconvolution transforms were performed using a Princeton Applied Research (PAR) Computer – controlled Potentiostat Model 283 and PAR Model 175 Universal Programer (from EG and G). The system allowed the use of any scan up to 100 V/s for the cyclic voltammetric experiment.

Measurements were made using a conventional three electrode cell configuration.. The platinum electrode surface was 7.85×10^{-3} cm^2 as a working electrode, coiled platinum wire as a counter electrode and saturated Ag/AgCl as a reference electrode.

The potential was calculated with relative to the Ag/AgCl reference electrode at 25°C and 0.1 mol/L tetraethylammonium chloride (*TEACl*) as background electrolyte. Cyclic voltammograms were recorded after background subtraction and iR compensation to minimize double-layer charging current and solution resistance. The working electrode was polished on a polisher Ecomet grinder. Cyclic voltammetric data were obtained at scan rate ranging from 0.02 to 5 V/s in non aqueous media at (25 ± 2) °C.

Digital simulation of the data for cyclic voltammetric experiments was performed on PC computer using EG & G condesim software package. The simulation procedure was carried out using finite differences techniques. Algorithms for the simulation program were coded and implemented into the condesim software package supplied by EG & G.

All working solutions were thoroughly degassed with oxygen free nitrogen and a nitrogen atmosphere was maintained above the solution throughout the experiments.

3. RESULTS AND DISCUSSION

3.1. Electro-oxidation Process

3.1.1. Cyclic voltammetric behavior

Cyclic voltammetry of 5 x 10^{-4} M of the investigated compound 4-[(anthracen -9-ylmethylene)-amino]-1, 5-dimethyl-2-phenyl-1,2-dihydro-pyrazol-3-one was measured in solvent, acetonitrile at scan rates ranging from 0.02— 5 V/s. Figure 1 gives an example of the cyclic voltammogram at sweep rate of 0.8 V/s. As shown in Figure 1, the first oxidative peak (A) was coupled with a small reductive peak (B) in the reverse scan, while the second oxidative

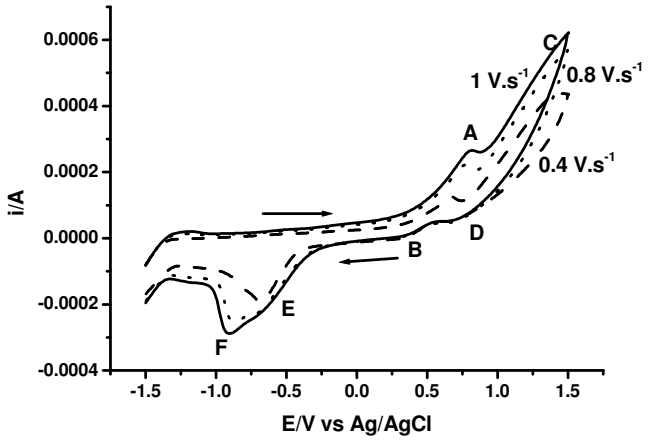

Figure 2. Cyclic voltammograms of 5×0^{-4} M of ***pyz*** in CH_3CN/0.1M TEACl at scan rate of 1 V/s (——), scan rate of 0.8 V/s (…….) and scan rate of 0.4 V/s (------).

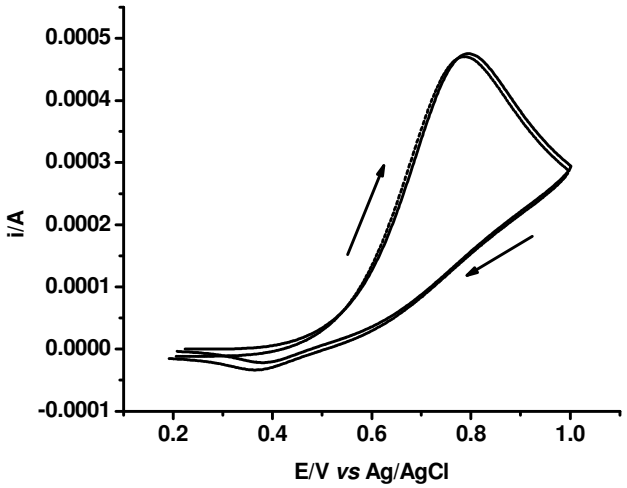

Figure 3. Matching between oxidative experimental voltammogram of ***pyz*** (———) and simulated voltammogram (--------) at a sweep rate of 0.1 V/s.

peak (C) was coupled with a small reductive peak (D) in the backward sweep.

It was found that the peak current increases with increasing the scan rate, while the forward anodic peak potentials of the oxidative processes were dependent on scan rate. From cyclic voltammetric investigation, it was found that, the anodic oxidative processes of the investigated pyrazole derivative proceeds as a slow charge transfer at all sweep rates. The absence of reductive peaks in the backward direction at low values of sweep rate confirm the presence of fast chemical step following the charge transfer. This behaviour demonstrates that the first charge transfer produces a cation radical followed by a fast chemical step and the radical cation loss another two electrons to form a trication which followed by fast chemical step. The ratio of the backward peak to the forward peak (i_pb/i_pf) is less than one for the two peaks, confirming the rapidity of the homogeneous chemical rate constant (k_c). Figure 2 displays the cyclic voltammograms at various scan rates. Inspection of Figure 2 revealed that, the oxidation peaks current, after elimination of the background current, is proportional to $v^{1/2}$, and the peak separation between the forward and backward peak potentials , ΔE_p, is dependent on the scan rate indicating the sluggish of charge transfer rate. Also, the measured values of peak width of the two waves, Ep – Ep/2 was found in the range of 0.174 - 0.412 ± 0.002 V, demonstrating the slow nature of the investigated system, where Ep and Ep/2 are the peak potential and the potential at the half- peak height respectively.

Again the peak separation ΔEp of the first and the second charge transfers was found to be in the range of 0.115 - 0.435 ± 0.005 V confirming the sluggish nature of charge transfer in 0.1 mol/L TEACl / CH_3CN. The redox potential (E^o) was determined from the mean position of the forward and backward peak potentials (Table 1). The standard heterogeneous rate constant (ks) cited in Table 1 was determined from the following equation [8].

$$k_s = 2.18 \left(\frac{D\alpha nFv}{RT}\right) \exp\left(-\frac{\alpha^2 nF}{RT}\Delta E_p\right) \quad (1)$$

Where ΔE_p is the peak separation and the other parameters have their usual meaning.

From the plot of i_p vs. $\sqrt{v}$, the diffusion coefficient (D) of the electroactive species was determined [9,10]. The calculated values of D are cited in Table 1. The results given in Figure 3 employ the

Table 1. Electrochemical parameters of the anodic oxidation processes of pyz compound

E^{o1} V	E^{o2} V	$k_{s1}\times10^5$ ms^{-1}	$k_{s2}\times10^6$ ms^{-1}	$D_1\times10^9$ m^2s^{-1}	$D_2\times10^9$ $m^2\,s^{-1}$	α_1	α_2	k_{c1}	k_{c2}
0.440[a]	1.120	1.70	8.20	1.10	2.76	0.30	0.31	6	-
0.451[b]	1.123	1.82	7.80	1.91	2.85	0.31	0.31	5.95	5.5
-[c]				1.66	2.50				
0.460[d]	1.121			1.23	2.54				
-[e]				1.16	2.62				
-[f]				1.34	2.51				

a) Experimental values, b) Simulated values, c) Values of D calculated via Eq.(5), d) Values calculated from Eq.(8), e) Values calculated from Cottrel plot, f) Values of D calculated from Eq.(12).

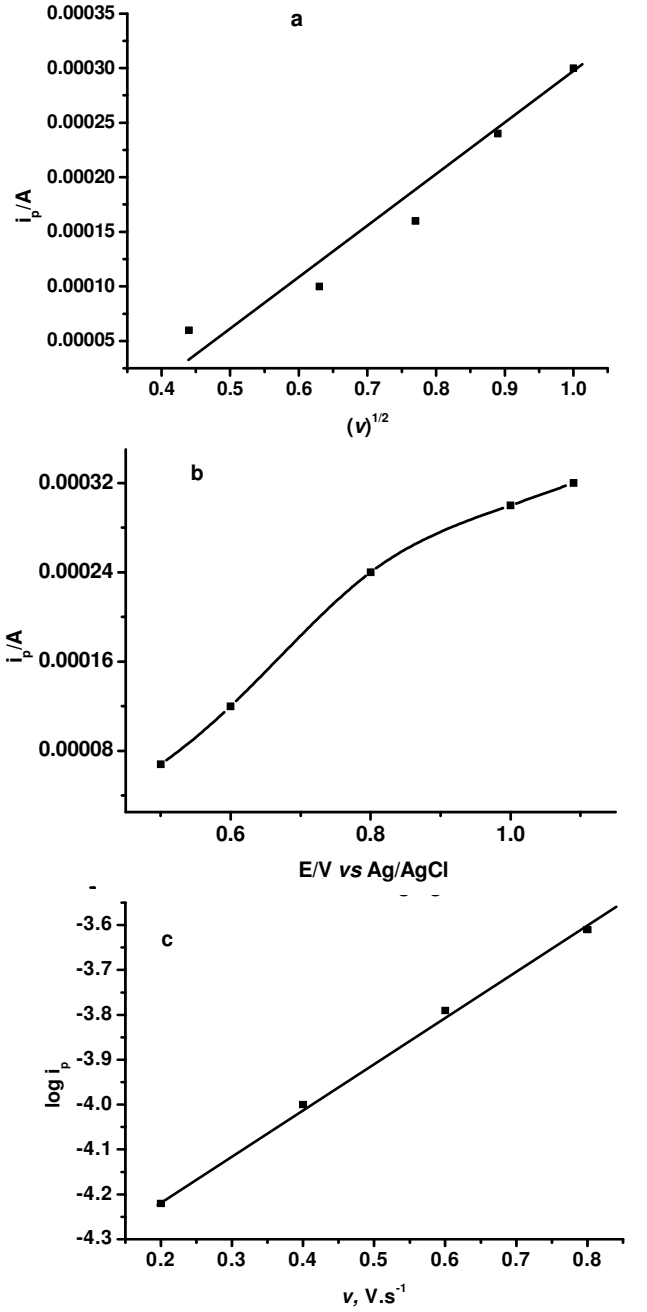

Figure 4. Effect of scan rate (*v*) on the oxidative peak current, (a) ip – √*v* relations, (b) ip – *v* √*v*. relations., (c) log i_p – *v* relations

experimental and theoretical values of the electrochemical parameters of the first peak of pyrazole derivative compound, which demonstrate good agreement between the captured and the simulated data. The effect of the scan rate (*v*) on peak current (i_p) of the first peak at a platinum electrode is shown in Figure 4. Though the i_p –*v* relation is curved, the i_p – $v^{1/2}$ and log i_p - *v* relations is linear, indicating that the current is diffusion-controlled [9].

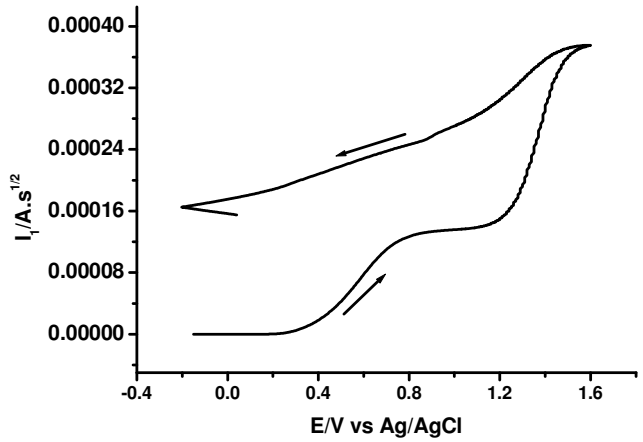

Figure 5. Convolution voltammetry (I_1) of the oxidative process of ***pyz*** at sweep rate of 0.2 V/s.

3.1.2. Convolution voltammetry

Convolution theorem finds use in the situation where it is required to perform the inverse transformation on a function which is the product of two functions of the Laplace variable each of which individually have known inverse transformations. In such a situation, the convolution theorem gives[11]:

$$L^{-1}[f_s(s).g_{s.}(s)] = \int_0^t G(u)F(t-u)du \quad (2)$$

in which f_s and g_s are the Laplace transform of the functions *F* and *G*, while the variables *u* is a dummy variable which is lost when the definite integral is evaluated.
For the reaction:

$$A + ne \rightleftharpoons B$$

in which a given species undergoing only electron transfer and no subsequent processes other than 'linear' diffusion out in the solution from a planar electrode, i.e. the Fick's second law is expressed as [12]:

$$[\partial C_A/\partial t]_x = D_A[\partial^2 C_A/\partial x^2]_x \quad (3)$$

Then the solution of the above via Laplace methods yielded

$$(C^{bulk} - C^s) = I_1 / nFSD^{1/2}{}_A \text{ and}$$
$$C^{bulk} = I_{lim} / nFSD^{1/2}{}_A \quad (4)$$

$$\text{i.e } I_{lim} = nFS\, C^{bulk} D^{1/2}{}_A \quad (5)$$

where C^{bulk} & C^s is the bulk and surface concentrations, respectively, and the convolution I_1 is given by $I_1 = i^*(\pi t)^{-1/2}$ or more 'fully' as:

$$I_1(t) = \pi^{-1/2} \int_0^t i(u) / (t-u)^{1/2} du \quad (6)$$

and I_{lim} is the limiting value of I_1 at 'extreme' potentials i.e. when the concentration at the electrode C^s is effectively reduced to zero

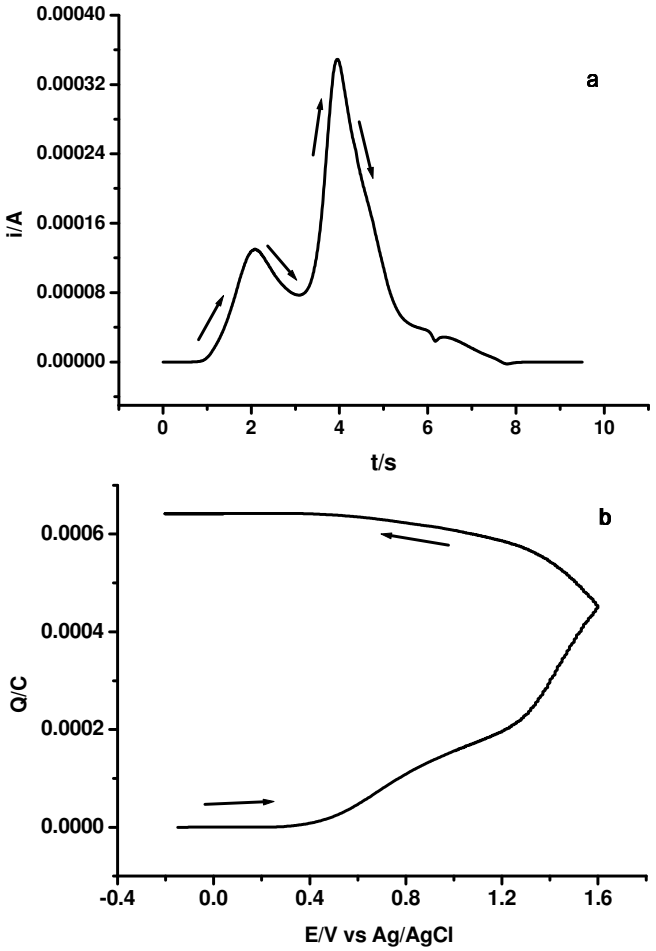

Figure 6. (a) plot of *i* versus *t* corresponding to a oxidative cyclic voltammogram at sweep rate of 0.1 V/s. The point $t = 5$ s is the time at which the potential scan is switched to the reverse direction, (b) plot of Q versus E.

by rapid redox conversion and the current is thus controlled solely by the maximum rates of diffusion to (and from) the electrode which allows to determine the diffusion coefficient of the bulk species [13-16].

Several algorithms have been proposed for the evaluation of the convolution integral *I(t)*. The following one was used in this work [17 – 22]:

$$I(t) = I(k\Delta t) = \frac{I}{\sqrt{\pi}} \sum_{j=1}^{j=k} \frac{\Gamma(k-j+1/2)}{(k-j)} \Delta t^{1/2} i(j\Delta t) \qquad (7)$$

where $I(j\Delta t)$ is the current read at equally spaced time intervals Δt and $\Gamma(x)$ is the Gamma function of x.

The values of the diffusion coefficients (D) corresponding to the oxidation steps were calculated via Eq. (5) and listed in Table 1. The I_1 convolution of the oxidative voltammogram at a scan rate of 0.2 V/s is indicated in Figure 5. As shown there is a large separation between the backward sweep and the forward sweep of the I_1 convolution. Also the backward sweep does not return to zero current value, confirming the presence of chemical step coupled with electron transfer and the slow kinetic of the heterogeneous rate constant (k_s) between the electrode and the electroactive pyrazole compound (***Pyz***), *i.e ECEEC* mechanism.

Also, the values of the diffusion coefficient were calculated from deduced convoluted current (I_{limd}) via the following relationship [10, 13]:

$$I_{\lim d} = \frac{i_p}{3.099\ (\alpha n_a \nu)^{1/2}} \qquad (8)$$

where I_{limd} is the deduced limiting convoluted current, which is defined as the limiting convoluted current . The values of diffusion coefficient calculated from I_{limd} agree well with the values calculated from cyclic voltammetry and convolutive voltammetry of the experimental voltammograms (Table 1).

The presentation of *i vs t* of the voltammogram at sweep rate of 0.1 V/s is shown in Fig 6a. The plot produces discontinuity Δi_c at t = 5 s due the reversibility of the scan. By selecting the data points a Cottrell plot are obtained as current versus the reciprocal square root of time. The slope of Cottrel plot yields a diffusion coefficient cited in Table 1. Inspection of Fig. 6a revealed that, the height of the first peak are nearly equal to the half height of the second peak, i.e the height of peak A is equal to the 1/2 height of peak C, the height of peak B is less than the height of peak A and the height of peak D is less than the height of peak C confirming that the number of electrons consumed in the second peak is double that consumed in the first peak, and also confirming the mechanistic *ECEEC* scheme of pyrazole derivative compound. The results shown in Fig. 6b represents the plot of charge versus potential which indicates that the anodic charges of the forward scan is unequal to the cathodic charges in the backward scan confirming the presence of chemical processes after the charges transfer [23].

3.1.3. Deconvolution transforms

Deconvolution of the current can be expressed as the differential of the I_1 convolution. In more general terms deconvolution is akin to semidifferentiation in a similar manner to considering $t^{-1/2}$ convolution as semiintegration. The relationship between $t^{-1/2}$ convolutions and deconvolutions is indicated in the following scheme [24].

$$dI_1/dt \underset{\text{deconvolution}}{\overset{\text{convolution}}{\rightleftharpoons}} i \underset{\text{deconvolution}}{\overset{\text{convolution}}{\rightleftharpoons}} I_1\,(t)$$

The deconvolution transforms of the current ($d\,I_1\,/dt$) as a function of E of reversible process is defined as [22]:

$$ep = (dI_1/dt) = nFAC\sqrt{D}\, a\zeta / (1+\zeta)^2 \qquad (9)$$

where

$$a = nvF/RT \qquad (10)$$

and

$$\zeta = exp\,[nF/RT\,(E - E^0)] \qquad (11)$$

and the representation of this equation at $v = 0.1$ *V/s* are indicated in Figure 7a.

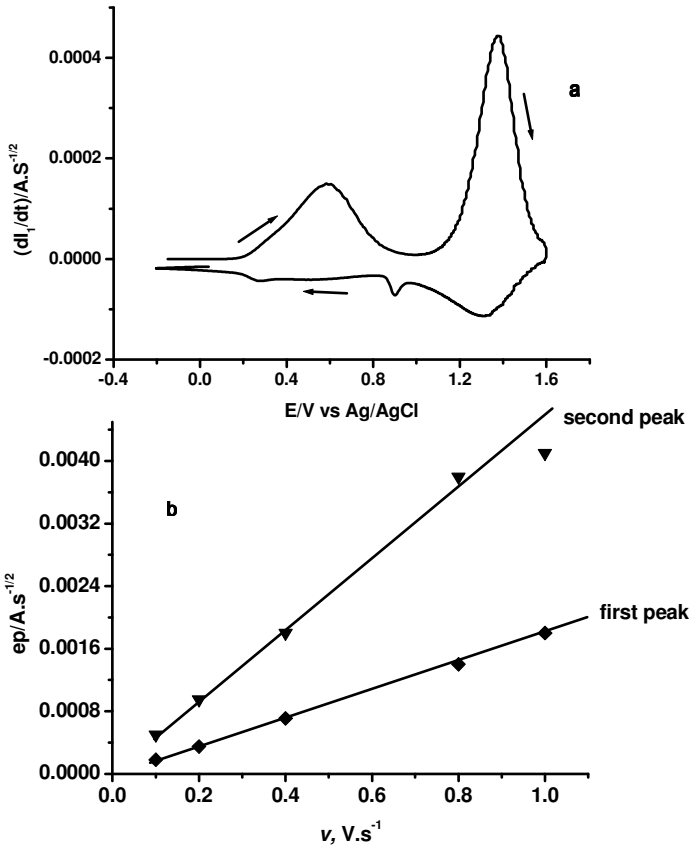

Figure 7. Deconvolution voltammetry (dI_1/dt) of the oxidative cyclic voltammogram of ***pyz*** at a sweep rate 0.1 V/s (a), e_p - v plot (b)

The asymmetry and the displacement of the forward and reverse sweep, further confirming the sluggish of electron transfer of *ECEEC* scheme of the oxidative processes of pyrazole derivative species. The standard reduction potentials were determined from the deconvoluted peak potentials of the two peaks (Table 1). The values of E^0_1 & E^0_2 determined from deconvolution voltammetry via Figure 7a compare well with the values calculated from cyclic voltammetry (Table 1).

The peak height of deconvoluted transforms is predicted to proportional to the concentration of the reducible species, to the electrode surface area, and to the scan rate v. The peak shape is very dependent on n, the number of electrons transferred, as n increase, the peak is predicted to become narrower and much higher. As indicated in Fig.7a the height of the first peak is nearly equal to half of the second one confirming the unequalty of the number of electrons consumed in both steps i.e the first one consumed one electron and the second one consumed two electrons. The diffusion coefficient (D) was also determined from deconvolution voltammetry using Eq. (12) [10 -13].

$$e_p = \frac{\alpha n^2 v C^{bulk} D^{1/2}}{3.367 RT} \qquad (12)$$

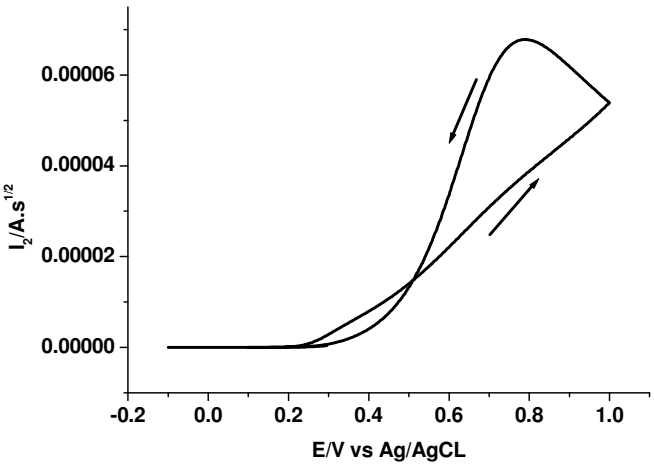

Figure 8. Kinetic convolution (I_2) of the first oxidation peak.

where e_p is the peak height (in ampere) of the forward deconvolution sweep and the remaining terms have their usual meanings. Values of the diffusion coefficient estimated by this method are given in Table 1.

Also from combination between convolution and deconvolution transforms, Eq. (13) was deduced [14]:

$$n = \frac{e_p\, 3.367\, RT}{\alpha F v I_{\lim}} \qquad n = \frac{0.086\, e_p}{I_{\lim} \alpha v} \qquad (13)$$

where n is the number of electrons consumed in the electrode reaction, and the other parameters have their usual definitions. From Eq. (13), the total number of electrons consumed in the electrode reaction was calculated and found to be 1.1 for the first wave and 2.02 for the second one i,e the total n is 3.12 (≈ 3). The successful determination of the number of electrons consumed in the electrode reaction using Eq. 13 without knowing the electrode surface area can be considered a simple and precise method for this purpose. The proportionalities of e_p with sweep rate v are presented and shown in Figure 7b. For both anodic peaks A and C the linearity is satisfactory and the lines pass through the origin confirming the diffusion controlled nature of the investigated species at a platinum electrode in 0.1 mol L^{-1} $TEACl/CH_3CN$ [13]. From the above discussion it was found that, the I_1 *vs* E and (dI_1/dt) *vs* E curves were easier to interpret than i *vs* E curve.

The kinetic convolution I_2 was used for the homogeneous chemical rate constant (k_c). The procedure was done via introducing various test values of k_c until a value is found that returns I_2 to zero at the end of the return sweep. Diagramatic examples of the function I_2 evaluated with the true value of k_c are shown in Fig. 8. The k_c true of the chemical step following the electron transfer is found to be 6 s^{-1} for the first step. The value of kc for the second step was determined via digital simulation method (Table 1).

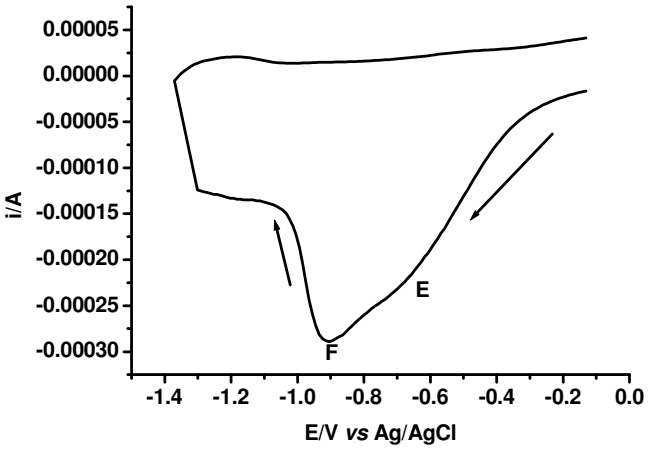

Figure 9. Reductive cyclic voltammograms of ***pyz*** in CH_3CN at scan rate of .06 V/s.

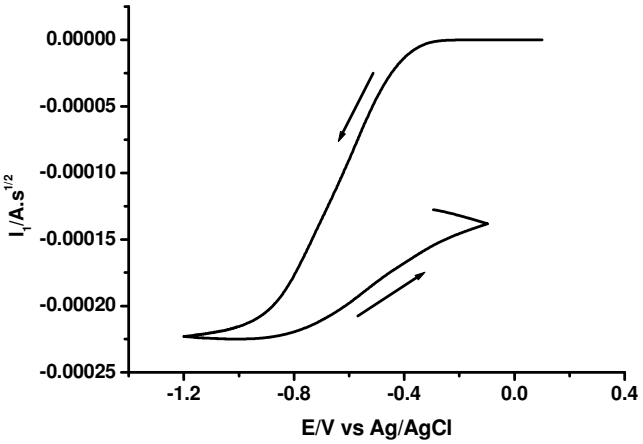

Figure 10. I_1 convolution transforms of reductive process of *pyz* at sweep rate of 0.6 V/s.

3.2. Electro-reduction process

3.2.1. Cyclic voltammetric behaviour

Electro-reduction of the investigated pyrazole derivatives compound ***pyz*** exhibited two reductive peaks with close two redox potentials. The first reductive peak (E) and the second one (F) is unidirectional at all sweep rates (0.02 - 5 V/s). An example response of the reductive cyclic voltammogram of ***Pyz*** compound at sweep rates of 0.8 V/s is illustrated in Fig. 9. The absence of the anodic peaks in backward direction give good evidence of ECEC scheme of the reduction process and also confirm the rapidity of the homogeneous chemical rate constant (k_c). Also the shift of peak potentials to more negative values with increasing the sweep rates reflect the sluggish of the rate of electron transfer.

The formal potentials (E^o_1 & E^o_2) and the standard heterogeneous rates constant (k_{s1} & k_{s2}) were calculated from digital simulation method and were listed in Table 2. Also, the diffusion coefficients (D_1 & D_2) were determined from the plot of $i_p - v^{1/2}$ and cited in Table 2.

3.2.2. Convolution-deconvolution transforms

In the case of slow rate of electron transfer, the diffusion coefficients (D_1 & D_2) of the investigated pyrazole compound ***pyz*** were determined from the following deduced limiting convoluted current equation (8). The calculated values of the diffusion coefficients (D_1 & D_2) were listed in Table 2. Figure 10 exhibits the I_1 convolution transforms of the reductive processes at 0.6 V/s indicating the slow nature of charge transfer processes and confirm the presence of chemical processes following the two charge transfer [13] i.e *ECEC* mechanism. The values of formal potentials (E^o_1 & E^o_2) were determined from the average peak positions of the deconvoluted voltammograms (Table 2).

The true kc values of the chemical process following the first and second charge transfer were determined from digital simulation and found 11.5 ± 0.05 s-1 and 9.6 ± 0.05 s-1 respectively Figure 11 shows an example of the comparison between the reductive experimental and the theoretical voltammograms of pyz compound at sweep rate of 1 V/s, which indicates an agreement between the two curves confirming the accuracy of the electrochemical parameters obtained from experimental cyclic voltammograms. The experimental and theoretical data of pyz compound were listed in Table 2.

The presentation of *i vs t* of the reductive cathodic voltammogram at sweep rate of 0.4 V/s is shown in Fig. 12. The plot produces discontinuity Δi_c at t = 2.5 s due to the reversibility of the scan. Inspection of Fig.12 revealed that, the inequality of the height of the forward and backward peaks, confirming that both

Table 2. Electrochemical parameters of the reduction process of ***pyz*** compound.

$-E^{o1}$ V	$-E^{o2}$ V	$k_{s1}\times10^5$ ms^{-1}	$k_{s2}\times10^5$ ms^{-1}	$D_1\times10^9$ m^2s^{-1}	$D_2\times10^9$ $m^2 s^{-1}$	α_1	α_2	k_{c1}	k_{c2}
-[a]	-	-	-	1.45	2.16	0.30	0.29	-	-
0.465[b]	0.648	3.92	2.55	1.60	2.15	0.31	0.30	11.1	9.60
-[c]	-	-	-	1.45	2.25				
0.459[d]	0.651	-	-	1.60	2.51				
-[e]	-	-	-	1.70	2.42				
-[f]	-	-	-	1.65	2.52				

a) Experimental values, b) Simulated values, c) Values of *D* calculated via Eq.(5), d) Values calculated from Eq.(8), e) Values calculated from Cottrel plot, f) Values of D calculated from Eq.(12).

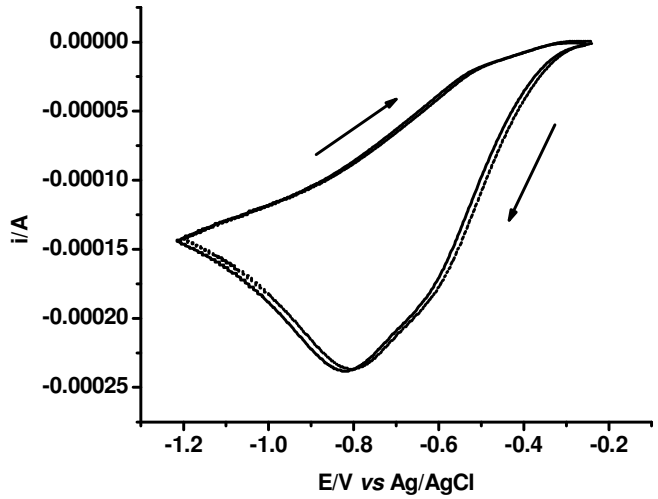

Figure 11. Matching between reductive experimental voltammogram of ***pyz*** (———) and simulated voltammogram (--------) at a sweep rate of 0.4 V/s.

charges transfer are followed by a chemical processes. By selecting the data points a cottrel plot is obtained as current versus the reciprocal square root of time. The slopes of Cottrell plots yield a diffusion coefficients D_1 & D_2 cited in Table 2.

The plot of the charge (Q) versus the potential (E) is shown in Fig.13 which reflects that the forward reductive charge is more than the backward oxidative charge confirming that the presence of a chemical processes after the charges transfer [25- 27].

From the above electrochemical studies the oxidative and reductive electrode pathway of 4-[(anthracen -9-ylmethylene)-amino]-1, 5-dimethyl-2-phenyl-1,2-dihydro-pyrazol-3-one (***pyz***) can be proposed to proceed as follows:

Oxidative process

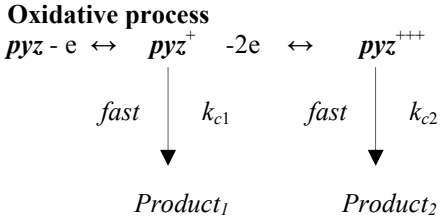

i.e. *ECEEC* mechanism

Reductive process

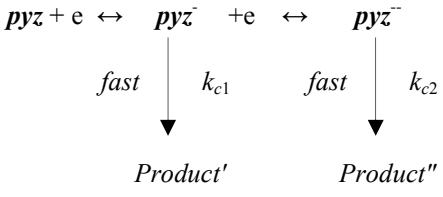

i.e. *ECEC* mechanism

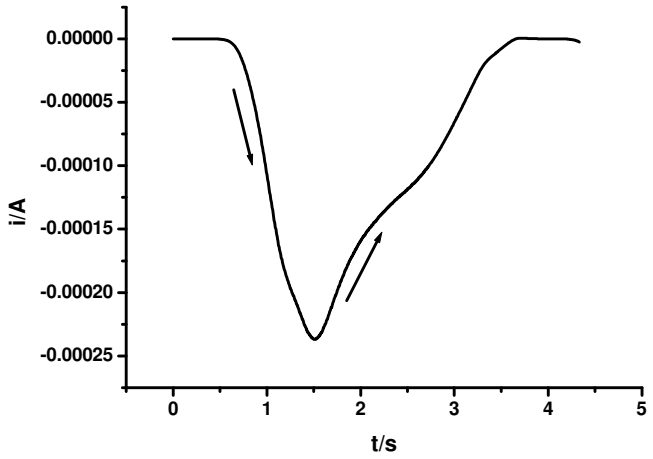

Figure 12. Plot of *i* versus *t* corresponding to reductive cyclic voltammogram at sweep rate of 0.4 V/s. The point t = 2.5 s is the time at which the potential scan is switched to the reverse direction.

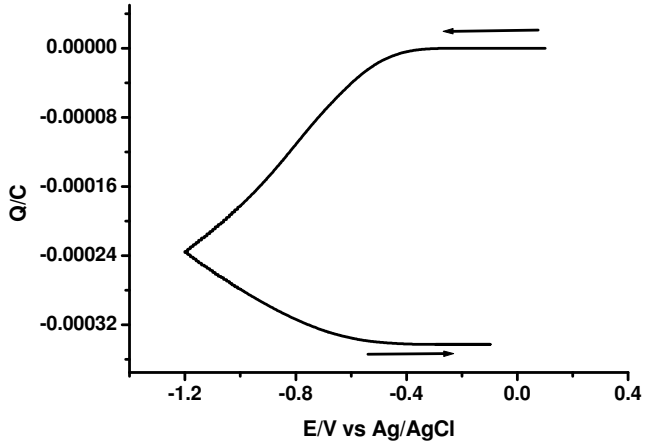

Figure 13. Plot of *Q* versus *E* corresponding to reductive cyclic voltammogram at sweep rate of 0.4 V/s.

4. CONCLUSION

The electrochemical behavior of anodic oxidation of ***pyz*** in 0.1 M TEACL /CH_3CN at a platinum electrode takes place as two oxidative peaks (A & C) coupled with two small reductive peaks (B & D) which appear only at high sweep rate > 1 V/s. This behavior demonstrates that the first charge transfer produces a radical cation that loss another two electrons to form a tri cation which proceed as *ECEEC*. Electro-reduction of ***pyz*** gave two cahodic peaks with close two redox potentials E^o_1 & E^o_2. The electrochemical parameters were determined experimentally and verified via a digital simulation method by comparing the generated theoretical voltammograms with the experimental voltammograms. The electrode reaction proceeds as *ECEC*.

REFERENCES

[1] Eicher T, Hauptmann S, Edition IInd, "The Chemistry of Heterocycles: Structure, Reactions, Syntheses, and Applications", Wiley-VCH, 2003.

[2] Katsunori K., Takayuki S., Hiromi I., JP 2002167305 (Konica Co., Japan), "Industrial antibacterial and antifungal agent with reduced human toxicity", 2002.

[3] Bailey J., J.Chem.Soc.Perkin Trans.I, 18, 2047 (1977).

[4] Bailey J., Bowes E., Marr P.A., Brit. 1247493, "Photographic colour processes", 1967.

[5] Diehl D.R., Mbiya K., Wray C.S., EP 20000628 (Eastman Kodak Co.USA), "Photographic element containing pyrazolazole coupler", 2001.

[6] Tawara K., Akira O., EP 0763569A1 (Konica Co.Japan), "Metal complex methin dye", 1997.

[7] Malinowska K, Gałecka E, Modranka R, Rutkowski M, Kedziora J.Pol. Merkur Lekarski, 24, 151 (2008).

[8] Klingler R.J.; Kochi J.K., J. Phys. Chem., 87, 1751 (1981).

[9] Nicholson R.S., Shain I., Anal. Chem., 37, 1351 (1965).

[10]El-Daly S.A., El-Hallag I.S., Ebeid E.M., Ghoneim M.M., Chin. J. Chem, 27, 241 (2009).

[11]Bowden W.J., J. Electrochem. Soc., 129, 1249 (1982).

[12]Wong E.H., Kabbani R.M., *Inorg. Chem*., 19, 451 (1980).

[13]El-Hallag I.S., Ghoneim M.M., Hammam E., *Anal. Chim. Acta,* 414, 173 (2000).

[14]Bard A.J., Faulkner L.R., Electrochemical Methods, Fundamentals and Applications, Wiley, New York, **1980**.

[15]El-Hallag I.S., Hassanien A.M., *Collect. Czech. Chem. Commun*., 64, 1953 (1999).

[16]El-Hallag I.S., Ghoneim M.M., *Monatsh. Chem*., 130, 525 (1999).

[17]Seidle A.R., Todd L., *J. Inorg. Chem*., 15, 2838 (1976).

[18]Hettrich R., Kaschke M., Wadepohl H., Weinmann W., Stephan M., Pritzkow H., Siebert W., Hyla-Kryspin I., Gleiter R., *Chem. Eur. J.*, 2, 487 (**1996).**

[19]Bould J., Kennedy J.D., Thornton-Pett M., *J. Chem. Soc. Dalton Trans*., 563 (1992).

[20]Stibr B., Kennedy J.D., Drdakova E., Thornton-Pett M., *J. Chem. Soc. Dalton. Trans*., 2335 (1993).

[21]Doetsch G., *Laplace Transformation*, Dover, New York, **1953**.

[22]Oldham K.B., Osteryoung R.A., J. Electroanal Chem., 11, 397 (1966).

[23]Galvez J., Park Su M., *J. Electroanal. Chem*., 235, 71 (1987).

[24]El-Hallag I.S., Ph.D. Thesis, Tanta University, Egypt, 1991.

[25]Al-bishri H.M., El-Hallag I.S., El-Mossalamy E.H., J. New. Mat. Electrochem. Systems, 14, 51 (2011).

[26]Asiri A.M., Khan S.A., El-Hallag I.S., J. New. Mat. Electrochem. Systems, In press.

[27]El-Hallag I.S., El-Daly S.A., Bull. Korean Chem. Soc., 31, 989 (2010).